Electronic Spectroscopy of Resonantly Stabilized Aromatic Radicals: 1-Indanyl and Methyl Substituted Analogues

Journal:	*The Journal of Physical Chemistry*
Manuscript ID:	jp-2015-05844q.R1
Manuscript Type:	Article
Date Submitted by the Author:	21-Jul-2015
Complete List of Authors:	Maity, Surajit; University of Basel, Chemistry Steglich, Mathias; university of basel, chemistry Maier, John; University of Basel, Department of Chemistry

Electronic Spectroscopy of Resonantly Stabilized Aromatic Radicals:

1-Indanyl and Methyl Substituted Analogues

Surajit Maity,* Mathias Steglich, John P. Maier*

Department of Chemistry, University of Basel, Klingelbergstrasse 80, CH 4056, Basel, Switzerland

Corresponding Authors: surajit.maity@gmail.com, j.p.maier@unibas.ch

Abstract

The gas-phase electronic spectra of two resonantly stabilized radicals, 1-indanyl (C_9H_9) and 1-methyl-1-indanyl ($C_{10}H_{11}$) have been recorded in the visible region using a resonant two-color two-photon ionization (R2C2PI) scheme. The $D_1(A'')\leftarrow D_0(A'')$ origin bands of 1-indanyl and 1-methyl-1-indanyl radicals are observed at 21157 cm^{-1} and 20565 cm^{-1}, respectively. The excitation of a′ vibrations in the D_1 state is observed up to ~1500 cm^{-1} above the origin band in both cases. The experimental assignments are in agreement with DFT and TD-DFT calculations. The R2C2PI spectrum recorded at m/z = 131 amu ($C_{10}H_{11}$) features three additional electronic transitions at 21433 cm^{-1}, 21369 cm^{-1} and 17989 cm^{-1}, which are assigned to the origin bands of 7-methyl-1-indanyl, 2,3,4-trihydronaphthyl and methyl-4-ethenylbenzyl radicals, respectively.

1. Introduction

Over the past decades, electronic spectroscopy of resonance-stabilized radicals (RSRs) has been the subject of interest among the atmospheric, astro- and combustion chemistry communities.[1-4] Due to a reduced decomposition rate and longer lifetime, RSRs were identified in a high concentration in combustion systems.[5-7] In the interstellar medium, RSRs are believed to play important roles in PAH formation at low temperatures due to barrierless radical-radical recombination reactions.[6-10] The aromatic counterparts of RSRs have not yet been identified in the ISM. However, they could contribute to the diffuse interstellar bands (DIB) because many of them possess electronic absorptions in the visible region.[1-4]

The present article focuses on the gas phase electronic spectra of the 1-indanyl radical (C_9H_9) and its methyl substituted analogue 1-methyl-1-indanyl radical ($C_{10}H_{11}$). Here, the radical center is located at α-position of the fused five-member carbon ring, which allows resonance stabilization via delocalization through π-orbitals of the benzene ring. The 1-indanyl radical was identified as the most stable isomer on the C_9H_9 potential energy surface.[11] In a previous study, the $D_1 \leftarrow D_0$ electronic excitation was observed in the 25000-20000 cm^{-1} region in a 3-methylhexane matrix at 77 K.[12] More recently, the origin band of this transition was identified in the gas phase at 21159 cm^{-1} utilizing R2C2PI, single vibronic level fluorescence (SVLF) and laser-induced fluorescence (LIF) spectroscopies.[4] The $D_0(A'')$ ground state was characterized based on the dispersed fluorescence data, but the vibrational progression excited in the $D_1(A'')$ state was not assigned. The electronic absorption and emission spectra were also reported in a neon matrix.[13] The $D_1(A'') \leftarrow D_0(A'')$ origin band was observed at 21235 cm^{-1}, shifted to the blue by 76 cm^{-1} compared to the gas phase. The electronic structure of another C_9H_9 isomer, 1-phenylallyl ($C_6H_5CHCHCH_2$) has also been

characterized by R2C2PI spectroscopy.[14,15] Among the $C_{10}H_{11}$ isomers, the gas phase electronic spectrum of 2,3,4-trihydronaphthyl radical was reported with the $D_1 \leftarrow D_0$ origin band at 21372 cm^{-1}.[16-18] However, an electronic spectrum of the most stable $C_{10}H_{11}$ isomer, 1-methyl-1-indanyl, has not been observed.

In this article, the R2C2PI scheme is utilized to investigate the $D_1 \leftarrow D_0$ electronic transition of 1-methyl-1-indanyl ($C_{10}H_{11}$). Assignments of the vibrations excited in the D_1 state of 1-indanyl (C_9H_9) are included. The analysis is supported by Franck-Condon and rotational profile simulations.

2. Method

2.1. Experimental

Electronic spectra of the gas phase radicals were recorded using an R2C2PI scheme coupled with a linear time-of-flight mass spectrometer (TOF-MS). The experiments were conducted in a three-stage differentially pumped vacuum chamber (~1.0×10^{-7} mbar) operational with turbo pumps. A gas mixture of 0.1 % propyne (C_3H_4) and 0.1 % diacetylene (C_4H_2) in helium (backing pressure 9 bar) was expanded by a pulsed valve (~220 μs) into the source chamber to maintain 4×10^{-5} mbar. Simultaneously, a pulsed (20Hz, 200 μs) electrical discharge (-500 to -600 V) was applied to the valve to produce the radicals. The molecular beam was collimated by passing through a 2.0 mm skimmer placed 50 mm downstream of the discharge source which passed between the extraction grids of the TOF-MS positioned inside the second chamber. A voltage of +300 V was applied to the skimmer to circumvent the incoming charged species produced in the discharge. A counter-propagating signal output of an optical parametric oscillator laser (5-10 ns; 20 Hz; 0.1 nm bandwidth, tuning range 410-710 nm, 2-8 mJ/pulse) excites the target radicals to higher electronic states. A subsequent fourth harmonic (266 nm) output of a Nd:YAG laser (3 mJ/pulse) was introduced about 2-4

ns after the excitation laser to ionize the radicals. The OPO is pumped by the third harmonic (355 nm) of the Nd:YAG laser that is also used to produce the 266 nm ionizing beam. This scheme eliminates temporal jitter between the pump and probe pulses.

The resulting ions were extracted perpendicular to the molecular beam into the TOF tube connected with a two-stage acceleration setup and finally detected by a micro-channel plate detector. Higher-resolution scans of the origin bands were carried out with a dye laser (≈ 10 ns; 10 Hz; 0.002 nm bandwidth) pumped by the third harmonic of an Nd:YAG laser. The dye laser output was calibrated with a wavelength meter. The pulsed valve, discharge and extraction voltage, and the laser pulses were synchronized by digital delay generators.

2.2. Theoretical

Calculations were carried out on various C_9H_9 and $C_{10}H_{11}$ isomers to aid spectral analysis. Density functional theory (DFT) and time-dependent DFT (TD-DFT) using the B3LYP functional and the 6-311++G(2d,p) basis set with Gaussian-09 package[19] were employed to predict geometries and harmonic frequencies in the ground and excited states. Vertical and adiabatic excitation energies and vertical ionization energies of the isomers were also calculated. Franck-Condon simulations were performed according to Barone et. al..[20] The rotational profiles were simulated with PGOPHER.[21]

3. Results

3.1. $D_1(A'')\leftarrow D_0(A'')$ Transition of C_9H_9 Radical

The R2C2PI spectrum of the C_9H_9 species recorded by monitoring the ion signal at m/z = 117 amu is shown in Figure 1. The strongest feature at 21157 cm^{-1} (472.5 nm) is assigned as the $D_1(A'')\leftarrow D_0(A'')$ origin band of 1-indanyl radical in agreement with the previously reported band at 21159 cm^{-1}.[4] The associated features in the blue region up to

~23000 cm^{-1} reveal a strong Franck-Condon activity. The energies of the observed bands and the excitation frequencies are listed in Table 1. In the previous study, three strong bands 677 cm^{-1}, 956 cm^{-1} and 1168 cm^{-1} to higher energy of the origin band were identified in both R2C2PI and LIF spectra.[4] These are in good agreement with the values 684 cm^{-1}, 964 cm^{-1} and 1166 cm^{-1} documented here (Table 1). In a neon matrix, two vibrational frequencies 683 cm^{-1} and 964 cm^{-1} in the D_1 state were also identified and assigned to ν_{28} and ν_{24} modes based on the calculated ground state values.[13] The high resolution scan of the $D_1(A'')\leftarrow D_0(A'')$ origin band is shown in Figure 2.

3.2. $D_1\leftarrow D_0$ Electronic Transitions of $C_{10}H_{11}$ Radicals

Figure 3 depicts the electronic excitation spectrum of $C_{10}H_{11}$ radicals recorded by monitoring the ion signal at m/z = 131 amu. The strongest band is at 20565 cm^{-1} (486.1 nm). Weaker features are observed in the high energy region up to 1600 cm^{-1}. A single band of a different transition is observed at 17989 cm^{-1} (555.7 nm). A new electronic spectrum of a $C_{10}H_{11}$ isomer is obtained; that of 2,3,4-trihydronaphthyl is known. The strongest band at 20565 cm^{-1} is assigned to the $D_1\leftarrow D_0$ origin band of the 1-methyl-1-indanyl radical (A). The band at 21369 cm^{-1} (467.8 nm) is most likely due to the $D_1\leftarrow D_0$ origin band of 2,3,4-trihydronaphthyl radical (F) in agreement with the reported value at 21372 cm^{-1}.[16-18] The feature at 17989 cm^{-1} possibly originates from a different isomer. Table 2 summarizes the vibrational frequencies for the $C_{10}H_{11}$ isomers inferred from the R2C2PI spectrum in the excited state. The high resolution recording of the band at 20565 cm^{-1} is shown in Figure 4.

4. Discussion

4.1. 1-Indanyl Radical

The origin band of the $D_1(A'')\leftarrow D_0(A'')$ electronic transition of 1-indanyl radical (C_9H_9-A, Table 3) is observed at 21157 cm^{-1}. This was established previously using LIF, SVLF spectroscopies and electronic structure calculation.[4] The four most stable C_9H_9 isomers are listed in Table 3. The second most stable isomer, C_9H_9-B (*trans*-phenylallyl radical), was reported to have the $D_1(A'')\leftarrow D_0(A'')$ origin band at 19208 cm^{-1}.[14] The electronic spectrum of *trans*-phenylallyl radical (C_9H_9-B) was observed up to 1650 cm^{-1} above the origin band. No bands were observed in the 21157 cm^{-1} - 22800 cm^{-1} region. The third isomer C_9H_9-C is expected to have the $D_1\leftarrow D_0$ system in the UV region. The first allowed transition is calculated at 3.88 eV (319 nm) (Table 3). In the case of the fourth isomer, C_9H_9-D, the calculated vertical ionization energy is high (7.8 eV), and cannot be ionized within the spectral range probed (21157 cm^{-1} - 22800 cm^{-1}). The above points lead to the conclusion that the band system shown in Figure 1 is due to the most stable isomer, 1-indanyl radical (C_9H_9-A).

Assignment of the vibrational frequencies is achieved through an agreement with the predicted Franck-Condon intensity pattern in the excited electronic state. As listed in Table 1, most of the vibrational bands up to 1500 cm^{-1} above the origin band are due to the low-energy totally symmetric modes (a′) of 1-indanyl radical in the D_1 state. In support of this, the scaled $(0.966)^{22}$ frequencies are within 10 to − 14 cm^{-1} of the experimental values given in Table 1. The experimental and calculated vibrational frequencies in the D_1 and D_0 states of 1-indanyl radical are compared in Table 4. The vibrations in the D_1 state are within 6 to − 52 cm^{-1} of the ground state frequencies (up to 1200 cm^{-1}).[4] This implies a small geometry change

upon electronic excitation. A change (−2.2 to 0.6 %) of the calculated rotational constants during $D_1 \leftarrow D_0$ transition supports this.

4.2. $D_1(A'') \leftarrow D_0(A'')$ origin band of 1-Indanyl

The high resolution scan of the origin band at 21157 cm^{-1} is shown in Figure 2 along with a rotational contour profile obtained using the calculated constants. A reasonable agreement is achieved using a hybrid *a/b* type transition with a ratio of 1.0 : 1.5. The choice of this ratio is obtained from the square of the transition dipole moments for the $D_1(A'') \leftarrow D_0(A'')$ transition. The calculated rotational constants of the D_0 and D_1 states of C_9H_9-A and simulation parameters are listed in Table 5. The origin band is ~8 cm^{-1} (T=18 K) wide with distinct P and R branches. Individual rotational lines are not resolved. This is due to the 0.08 cm^{-1} resolution of the scanning laser because the lifetime of the D_1 state was estimated to be in the order of μs.[4]

4.3. Identification of $C_{10}H_{11}$ Isomers

To identify the specific $C_{10}H_{11}$ isomer with origin band at 20565 cm^{-1} (Figure 3), DFT and TD-DFT calculations were performed (Table 6). Selective minima among the following structural groups are listed: (i) five most stable structures ($C_{10}H_{11}$-A,B,C,D and E) of methyl substituted indanyl radicals, (ii) one hydrogenated naphthyl radical ($C_{10}H_{11}$-F), two lowest energy (iii) methyl substituted phenylallyl radicals ($C_{10}H_{11}$-G and H) and (iv) methyl substituted 4-ethenyl benzyl radicals ($C_{10}H_{11}$-I and J). The 1-methyl-1-indanyl radical ($C_{10}H_{11}$-A) is the most stable isomer. However, the relative energies of the substituted indanyl isomers (group (i): $C_{10}H_{11}$-B,C,D and E) and hydrated naphthyl radical (group (ii): $C_{10}H_{11}$-F) are calculated within 6-16 kJ mol^{-1} above $C_{10}H_{11}$-A. The structure $C_{10}H_{11}$-F can be excluded because the origin band of its $D_1 \leftarrow D_0$ transition is identified at 21372 cm^{-1}.[16-18] Each of the other structures has an ionization potential (Table 6) less than the experimental

limit of 7.21 eV. Based on the stabilization energies and ionization potentials, an unambiguous assignment is hard to achieve. Only the higher energy structures belonging to groups (iii) and (iv) can be excluded because Franck-Condon simulations are in poor agreement with the experimental data (Supporting Information Figure S1).

4.3.1. 1-Methyl-1-indanyl Radical

A methyl versus atomic hydrogen substitution to 1-indanyl radical ($C_9H_9 \rightarrow C_{10}H_{11}$) is expected to lower the $D_1 \leftarrow D_0$ transition energy. In support, the $D_1 \leftarrow D_0$ electronic transitions of a series of methyl substituted benzyl radicals are related with red shifted origin bands compared to the parent benzyl radical.[23,24] The origin bands of 2-methyl-, 3-methyl-, 4-methyl- and α-methyl- benzyl radicals (C_8H_9) are shifted to the red by 656, 516, 302 and 224 cm^{-1}, respectively, compared to that of the bare benzyl radical at 22002 cm^{-1}.[23,24] A similar effect upon methyl substitution is expected for the 1-indanyl radical. The band at 20565 cm^{-1} (Figure 3) lies 592 cm^{-1} to the red of the $D_1 \leftarrow D_0$ origin of C_9H_9-A. Hence, it may be assigned to a methyl substituted 1-indanyl radical considering the stability of these isomers.

The calculated $D_1 \leftarrow D_0$ vertical excitation energies of the structures $C_{10}H_{11}$-A,B,C,D, and E are 0.34-0.47 eV higher than the experimental origin band at 2.55 eV (486.1 nm), the closest being $C_{10}H_{11}$-A. The calculated adiabatic excitation energies show a better agreement. The predicted energies of $C_{10}H_{11}$-A,B,C,D, and E isomers (478, 458, 452, 473 and 453 nm) are estimated 0.04-0.19 eV above the observed energy, with again $C_{10}H_{11}$-A displaying the best match. As $C_{10}H_{11}$-A is also the most stable $C_{10}H_{11}$ isomer, it is suggested as the carrier of the electronic transition starting at 20565 cm^{-1}. In support of this, a Franck-Condon analysis was conducted for the $D_1 \leftarrow D_0$ band system of $C_{10}H_{11}$-A and the predicted intensity pattern is shown in Figure 3. Except for the strong bands at 21369 cm^{-1} and 21433 cm^{-1}, most observed bands can be reproduced. The vibrational bands (Table 2) are assigned to the low-energy in-

plane vibrations (a′) in the D_1 state of $C_{10}H_{11}$-A. The bands 244, 418 and 480 cm^{-1} above the origin are due to the excitation of the three lowest-energy in-plane vibrations ν_{36}, ν_{35}, ν_{34}. Similar vibrational modes are identified in the D_1 state of 1-indanyl radical. For example, the ν_{35} and ν_{34} modes of 1-methyl-1-indanyl ($C_{10}H_{11}$-A) are almost identical with ν_{31}, ν_{30} of 1-indanyl (C_9H_9-A).

Figure 4 shows the high resolution scan of the origin band 21157 cm^{-1}. It is ~5 cm^{-1} wide and features distinct P and R branches. A rotational contour fit based on the calculated rotational constants of $C_{10}H_{11}$-A in D_0 and D_1 states is compared with the experimental spectrum. In this, a mixed 1:2 *a/b* type transition is considered. The ratio is obtained in a similar way as discussed in section 4.2. A reasonable agreement is achieved at a rotational temperature of 15 K. However, the high resolution scan can also be reproduced using the rotational constants of the other methyl substituted 1-indanyl radicals ($C_{10}H_{11}$-B, C, D and E) (SI). Individual rotational lines are not resolved, most likely due to the 0.08 cm^{-1} resolution of the scanning laser.

4.3.2. Other $C_{10}H_{11}$ Isomers

The bands at 17989 cm^{-1}, 21369 cm^{-1}, and 21433 cm^{-1} do not agree with the Franck-Condon simulation for the 1-methyl-1-indanyl radical $C_{10}H_{11}$-A. Other isomers are likely to contribute.

2,3,4-trihydronaphthyl radical ($C_{10}H_{11}$-F): The observed band at 21369 cm^{-1} (Figure 3) is assigned to the $D_1 \leftarrow D_0$ transition of $C_{10}H_{11}$-F based on the agreement with the literature data.[16-18] The isomer $C_{10}H_{11}$-F is only 6 kJ mol^{-1} less stable than the lowest energy structure $C_{10}H_{11}$-A and formation in the discharge source is likely. No additional bands could be linked to this isomer because the origin band at 21369 cm^{-1} is weak. Any associated vibrational transitions are likely to be within the noise level of the spectrum.

7-methyl-1-indanyl radical ($C_{10}H_{11}$-B): The band at 21433 cm^{-1} lies 868 cm^{-1} to higher energy of the $D_1 \leftarrow D_0$ origin band of $C_{10}H_{11}$-A. This can be assigned to the $D_1 \leftarrow D_0$ transition of another methyl substituted 1-indanyl radical ($C_{10}H_{11}$-B,C,D and E) because the calculated vertical excitation energies are slightly higher (0.04-0.17 eV) than for $C_{10}H_{11}$-A. The calculated adiabatic excitation energies of $C_{10}H_{11}$-B (2.71eV) and $C_{10}H_{11}$-D (2.62 eV) are close to the experimental value of 2.66 eV. $C_{10}H_{11}$-B is also the second most stable structure among the methyl substituted indanyl radicals (Group (i)) and is about 6 kJ mol^{-1} less stable than $C_{10}H_{11}$-A. An additional band observed at 21888 cm^{-1}, corresponding to a vibrational frequency 455 cm^{-1} is in agreement with the value 464 cm^{-1} of the ν_{34} mode of $C_{10}H_{11}$-B. One of the most intense vibrational bands in the spectrum (Figure 3) of 1-methyl-1-indanyl radical ($C_{10}H_{11}$-A) is also ν_{34} at 480 cm^{-1}.

Substituted benzyl radical ($C_{10}H_{11}$-I and J): The band at 17989 cm^{-1} is tentatively assigned to an electronic transition due to the group (iv) radicals i.e. $C_{10}H_{11}$-I and J (methyl substituted 4-ethenyl-benzyl). The isomers $C_{10}H_{11}$-I and J are the least stable structures with stabilization energies of 48 and 52 kJ mol^{-1} higher than $C_{10}H_{11}$-A. The proposed assignment is exclusively based on a comparison of the calculated adiabatic excitation energies. Those are of $C_{10}H_{11}$-I (2.33 eV) and $C_{10}H_{11}$-J (2.30 eV) in good agreement with the observed value at 2.23 eV. The formation of less stable isomers cannot be excluded in the discharge source.

5. Summary

The gas phase electronic transitions of 1-indanyl radical (C_9H_9) and its methyl substituted analogues ($C_{10}H_{11}$) have been measured using a R2C2PI spectroscopic method. The $D_1 \leftarrow D_0$ band system of 1-indanyl radical (C_9H_9) is identified. The inferred vibrational frequencies in the excited D_1 state are in agreement with the calculated totally symmetric modes in the D_1 state. The $D_1 \leftarrow D_0$ electronic transition of 1-methyl-1-indanyl radical

($C_{10}H_{11}$) is observed for the first time with origin band at 20565 cm^{-1}. In the D_1 state, totally symmetric vibrations up to 1500 cm^{-1} are identified. Other $C_{10}H_{11}$ isomers, the 7-methyl-1-indanyl radical ($C_{10}H_{11}$-B) and methyl substituted 4-ethenyl benzylic radicals ($C_{10}H_{11}$-I/ $C_{10}H_{11}$-J) are tentatively assigned with $D_1 \leftarrow D_0$ origin bands at 21433 and 17989 cm^{-1}, respectively.

Supporting Information Available. Rotational constants, simulated rotational profiles (both *a*- and *b*-type) and Franck-Condon simulations of $D_1 \leftarrow D_0$ electronic transitions for $C_{10}H_{11}$ isomers are given. Estimation of the scaling factor of 1-indanyl radical in the excited state is discussed as well. This material is available free of charge via the Internet at http://pubs.acs.org.

Acknowledgement

This work is funded by Swiss National Science Foundation (Project 200020-140316/1)

References

(1) Ding, H.; Schmidt, T. W.; Pino, T.; Boguslavskiy, A. E.; Guthe, F.; Maier, J. P. Gas Phase Electronic Spectra of the Linear Carbon Chains $HC_{2n+1}H$ (n=3-6,9), *J. Chem. Phys.* **2003**, *119*, 814-819.
(2) Reilly, N. J.; Kokkin, D. L.; Nakajima, M.; Nauta, K.; Kable, S. H.; Schmidt, T. W. Spectroscopic Observation of the Resonance-Stabilized 1-Phenylpropargyl Radical, *J. Am. Chem. Soc.* **2008**, *130*, 3137-3142.
(3) Reilly, N. J.; Nakajima, M.; Gibson, B. A.; Schmidt, T. W.; Kable, S. H. Laser-induced Fluorescence and Dispersed Fluorescence Spectroscopy of Jet-cooled 1-Phenylpropargyl Radical, *J. Chem. Phys.* **2009**, *130*, 144313.
(4) Troy, T. P.; Nakajima, M.; Chalyavi, N.; Clady, R. G. C. R.; Nauta, K.; Kable, S. H.; Schmidt, T. W. Identification of the Jet-Cooled 1-Indanyl Radical by Electronic Spectroscopy, *J. Phys. Chem. A* **2009**, *113*, 10279-10283.
(5) Kern, R. D.; Singh, H. J.; Wu, C. H. Thermal Decomposition of 1,2 Butadiene, *Int. J. Chem. Kinet.***1988**, *20*, 731-747.
(6) McEnally, C. S.; Pfefferle, L. D.; Atakan, B.; Kohse-Hoinghaus, K. Studies of Aromatic Hydrocarbon Formation Mechanisms in Flames: Progress towards Closing the Fuel Gap, *Prog. Energy Combust. Sci.* **2006**, *32*, 247-294.

(7) Miller, J. A.; Melius, C. F. Kinetic and Thermodynamic Issues in the Formation of Aromatic Compounds in Flames of Aliphatic Fuels, *Combust. Flame* **1992**, *91*, 21-39.
(8) da Silva, G.; Bozzelli, J. W. The C_7H_5 Fulvenallenyl Radical as a Combustion Intermediate: Potential New Pathways to Two- and Three-Ring PAHS, *J. Phys. Chem. A* **2009**, *113*, 12045-12048.
(9) Djokic, M. R.; Van Geem, K. M.; Cavallotti, C.; Frassoldati, A.; Ranzi, E.; Marin, G. B. An Experimental and Kinetic Modeling Study of Cyclopentadiene Pyrolysis: First Growth of Polycyclic Aromatic Hydrocarbons, *Combust. Flame* **2014**, *161*, 2739-2751.
(10) D'Anna, A.; D'Alessio, A.; Kent, J. A Computational Study of Hydrocarbon Growth and the Formation of Aromatics in Coflowing Laminar Diffusion Flames of Ethylene, *Combust. Flame* **2001**, *125*, 1196-1206.
(11) Vereecken, L.; Peeters, J.; Bettinger, H. F.; Kaiser, R. I.; Schleyer, P. v. R.; Schaefer, H. F. Reaction of Phenyl Radicals with Propyne, *J. Am. Chem. Soc.* **2002**, *124*, 2781-2789.
(12) Izumida, T.; Inoue, K.; Noda, S.; Yoshida, H. Electronic Spectra of Some Aromatic Free Radicals, *Bull. Chem. Soc. Jpn.* **1981**, *54*, 2517-2518.
(13) Nagy, A.; Garkusha, I.; Fulara, J.; Maier, J. P. Electronic Spectroscopy of Transient Species in Solid Neon: the Indene-motif Polycyclic Hydrocarbon Cation Family $C_9H_y^+$ (y = 7-9) and Their Neutrals, *Phys. Chem. Chem. Phys.* **2013**, *15*, 19091-19101.
(14) Troy, T. P.; Chalyavi, N.; Menon, A. S.; O'Connor, G. D.; Fuckel, B.; Nauta, K.; Radom, L.; Schmidt, T. W. The Spectroscopy and Thermochemistry of Phenylallyl Radical Chromophores, *Chem. Sci.* **2011**, *2*, 1755-1765.
(15) Sebree, J. A.; Kidwell, N. M.; Buchanan, E. G.; Zgierski, M. Z.; Zwier, T. S. Spectroscopy and Ionization Thresholds of π-Isoelectronic 1-Phenylallyl and Benzylallenyl Resonance Stabilized Radicals, *Chem. Sci.* **2011**, *2*, 1746-1754.
(16) Kidwell, N. M.; Mehta-Hurt, D. N.; Korn, J. A.; Sibert, E. L.; Zwier, T. S. Ground and Excited State Infrared Spectroscopy of Jet-cooled Radicals: Exploring the Photophysics of Trihydronaphthyl and Inden-2-ylmethyl, *J. Chem. Phys.* **2014**, *140*, 214302.
(17) Sebree, J. A.; Kislov, V. V.; Mebel, A. M.; Zwier, T. S. Isomer Specific Spectroscopy of $C_{10}H_n$, n = 8-12: Exploring Pathways to Naphthalene in Titan's Atmosphere, *Farad. Discuss.* **2010**, *147*, 231-249.
(18) Sebree, J. A.; Kislov, V. V.; Mebel, A. M.; Zwier, T. S. Spectroscopic and Thermochemical Consequences of Site-Specific H-Atom Addition to Naphthalene, *J. Phys. Chem. A* **2010**, *114*, 6255-6262.
(19) Frisch, M. J.; Trucks, G. W.; Schlegel, H. B.; Scuseria, G. E.; Robb, M. A.; Cheeseman, J. R.; Scalmani, G.; Barone, V.; Mennucci, B.; Petersson, G. A. et. al. Gaussian 09; Gaussian, Inc.: Wallingford, CT, USA, 2009.
(20) Barone, V.; Bloino, J.; Biczysko, M. Vibrationally-resolved Electronic Spectra in GAUSSIAN 09, 2009.
(21) Western, C. M. PGOPHER, A Program for Simulating Rotational Structure, University of Bristol, http://pgopher.chm.bris.ac.uk, 2014.
(22) See Supporting Information.
(23) Lee, S. K.; Ahn, B. U.; Lee, S. K. Vibronic Spectrum of the Jet-cooled 2, 6-Dimethylbenzyl Radical in a Corona Excitation, *J. Phys. Chem. A* **2003**, *107*, 6554-6557.
(24) Lee, G. W.; Ahn, H. G.; Kim, T. K.; Lee, S. K. Spectroscopic Evidence of α-Methylbenzyl Radical in the Gas Phase, *Chem. Phys. Lett.* **2008**, *465*, 193-196.

Table of Contents

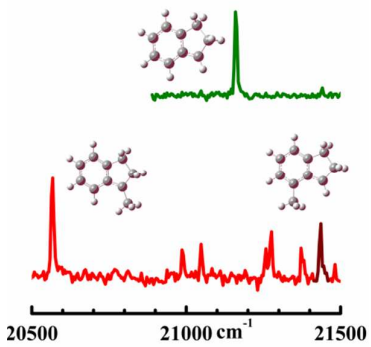

Table 1. Observed absorption bands in the $D_1(A'')\leftarrow D_0(A'')$ transition of 1-indanyl radical (C_9H_9) and assignment. Literature values are given in bold italics.[13]

λ (nm)	ν (cm^{-1})	Δν (cm^{-1})	Assignment	Calculated Frequencies (cm^{-1})	
				Unscaled	× 0.966
472.5	21157	0	0_0^0		
466.3	21438	281	$47_0^2(?)$		
464.7	21512	355	31_0^1	369	356
461.8	21647	490	30_0^1	506	489
460.8	21694	537	29_0^1	562	543
457.7	21841	684 (***683***)	28_0^1	702	678
457.1	21869	712	$30_0^2(?)$		
456.2	21912	755	27_0^1	792	765
454.9	21975	818	$31_0^1 30_0^1(?)$		
453.8	22028	871	25_0^1	905	874
452.5	22092	935	..		
451.9	22121	964 (***964***)	24_0^1	985	952
448.2	22303	1146	…		
447.8	22323	1166	19_0^1	1201	1160
447.1	22358	1201	18_0^1	1241	1199
446.5	22388	1231	17_0^1	1284	1240
446.1	22408	1251	…		
445.6	22434	1277	16_0^1	1326	1281
444.1	22509	1352	13_0^1,14_0^1, $28_0^2(?)$	1403, 1425	1355, 1377
442.3	22601	1444	10_0^1	1475	1425

441.4	22647	1490	9_0^1	1531	1480
441.1	22662	1505	8_0^1	1570	1516

Table 2. Observed absorption bands of $C_{10}H_{11}$ isomers along with assignments (tentative for $C_{10}H_{11}$-B and $C_{10}H_{11}$-I/J)

λ (nm)	ν (cm^{-1})	Δν (cm^{-1})	Assignment	Calculated Frequencies (cm^{-1})
$C_{10}H_{11}$-A ($D_1(A'')\leftarrow D_0(A'')$)				
486.1	20565	0	0_0^0	
480.4	20809	244	36_0^1	256
476.4	20983	418	35_0^1	433
475.0	21045	480	34_0^1	511
470.3	21256	691	?	...
469.9	21274	709	31_0^1	722
465.4	21479	914	$[28_0^1, 27_0^1]$	986, 988
462.3	21623	1058	26_0^1	1056
459.9	21736	1171	22_0^1	1197
451.6	22136	1571	9_0^1	1559
$C_{10}H_{11}$-B ($D_1(A'')\leftarrow D_0(A'')$)				
466.4	21433	0	0_0^0	...
456.7	21888	455	34_0^1	464
$C_{10}H_{11}$-F ($D_1(A)\leftarrow D_0(A)$)				
467.8	21369	0	0_0^0	...
$C_{10}H_{11}$-I/J ($D_1(A'')\leftarrow D_0(A'')$)				
555.7	17989	0	0_0^0	...

Table 3. Relative stabilities (E) and vertical ionization energies (IP) of C_9H_9 isomers calculated at the B3LYP/6-311++g(2d,p) level. Vertical excitation energies (ΔE) of $D_{1\text{-}3} \leftarrow D_0$ transitions along with oscillator strength (*f*) calculated with TD-B3LYP/6-311++g(2d,p) theory. Calculated adiabatic excitation energies are given in bold italics.

		E (kJ mol^{-1})	IP (eV)	ΔE		*f*
				Transitions	eV (nm)	
C_9H_9-A	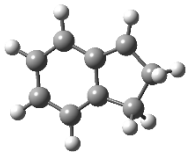	0	6.5	$D_1(A'') \leftarrow D_0(A'')$	3.00 (413, ***456***)	0.0029
				$D_2(A'') \leftarrow D_0(A'')$	3.37 (367)	0.0002
				$D_3(A'') \leftarrow D_0(A'')$	3.70 (335)	0.0254
C_9H_9-B	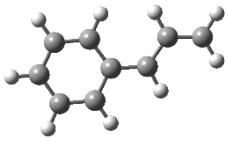	18	6.8	$D_1(A'') \leftarrow D_0(A'')$	2.86 (433, ***469***)	0.0007
				$D_2(A'') \leftarrow D_0(A'')$	3.26 (380)	0.0027
				$D_3(A'') \leftarrow D_0(A'')$	3.68 (337)	0.0291
C_9H_9-C	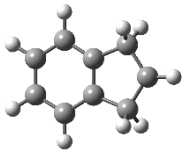	43	7.4	$D_1(A_1) \leftarrow D_0(B_1)$	3.88 (319, ***375***)	0.0016
				$D_2(B_1) \leftarrow D_0(B_1)$	4.13 (300)	0.0000
				$D_3(A_2) \leftarrow D_0(B_1)$	4.17 (297)	0.0001
C_9H_9-D	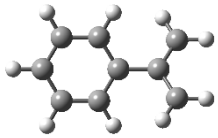	52	7.8	$D_1(B) \leftarrow D_0(A)$	3.06 (405, ***471***)	0.0029
				$D_2(B) \leftarrow D_0(A)$	3.91 (317)	0.0248
				$D_3(A) \leftarrow D_0(A)$	3.94 (315)	0.0001

Table 4. Experimental and calculated vibrational frequencies in cm^{-1} in $D_1(A'')$ and $D_0(A'')$ states of 1-indanyl radical (C_9H_9-A). The experimental values for the ground state are taken from reference 4. The calculated frequencies are scaled by factors of 0.966 (D_1) and 0.981 (D_0).[22]

Mode	$D_1(A'')$	Experimental	$D_0(A'')$	Experimental
ν_{31}	356	355	377	377
ν_{30}	489	490	526	529
ν_{29}	543	537	581	583
ν_{28}	678	684	699	700
ν_{27}	765	755	792	794
ν_{25}	874	871	903	865
ν_{24}	952	964	1013	1016
ν_{19}	1160	1166	1224	1211
ν_{18}	1199	1201	1183	1183

Table 5. Calculated rotational constants (cm^{-1}) in $D_0(A'')$ and $D_1(A'')$ states of 1-indanyl and 1-methyl-1-indanyl radicals and simulation parameters.

	1-indanyl		1-methyl-1-indanyl	
Origin	21157.3±0.1		20565.3±0.1	
Band type	*a/b*=2/3		*a/b*=1/2	
T	~18		~15	
Rotational Constants	$D_0(A'')$	$D_1(A'')$	$D_0(A'')$	$D_1(A'')$
A	0.122	0.119	0.081	0.080
B	0.050	0.051	0.041	0.042
C	0.036	0.036	0.028	0.028

Table 6. Relative stabilities (E) and vertical ionization energies (IP) of $C_{10}H_{11}$ isomers calculated with B3LYP/6-311++g(2d,p) theory. The vertical excitation energies (ΔE) of D_{1-3}←D_0 transitions along with oscillator strength (*f*) calculated with TD-B3LYP/6-311++g(2d,p). Adiabatic excitation energies are given in bold italics.

		E (kJ mol^{-1})	IP (eV)	ΔE		*f*
				Transitions	eV (nm)	
$C_{10}H_{11}$-A	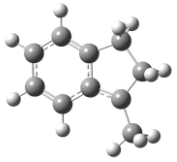	0	5.91	$D_1(A'')$←$D_0(A'')$	2.89 (429, ***478***)	0.0040
				$D_2(A'')$←$D_0(A'')$	3.35 (370)	0.0041
				$D_3(A')$←$D_0(A'')$	3.39 (366)	0.0027
$C_{10}H_{11}$-B	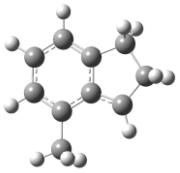	6	6.08	$D_1(A'')$←$D_0(A'')$	2.99 (415, ***458***)	0.0003
				$D_2(A'')$←$D_0(A'')$	3.34 (372)	0.0019
				$D_3(A'')$←$D_0(A'')$	3.55 (349)	0.0391
$C_{10}H_{11}$-C	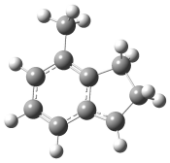	8	6.12	$D_1(A'')$←$D_0(A'')$	3.01 (411, ***452***)	0.0002
				$D_2(A'')$←$D_0(A'')$	3.36 (369)	0.0038
				$D_3(A'')$←$D_0(A'')$	3.57 (347)	0.0259
$C_{10}H_{11}$-D	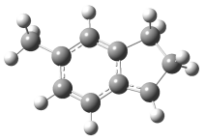	8	5.99	$D_1(A'')$←$D_0(A'')$	2.92 (425, ***473***)	0.0052
				$D_2(A'')$←$D_0(A'')$	3.29 (377)	0.0003
				$D_3(A'')$←$D_0(A'')$	3.58 (347)	0.0000
$C_{10}H_{11}$-E	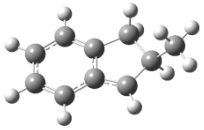	16	6.47	$D_1(A)$←$D_0(A)$	3.02 (411, ***453***)	0.0026
				$D_2(A)$←$D_0(A)$	3.36 (369)	0.0003
				$D_3(A)$←$D_0(A)$	3.61 (344)	0.0212
$C_{10}H_{11}$-F	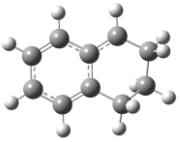	6	6.25	$D_1(A)$←$D_0(A)$	3.06 (405)	0.0006
				$D_2(A)$←$D_0(A)$	3.33 (372)	0.0010
				$D_3(A)$←$D_0(A)$	3.64 (341)	0.0225
$C_{10}H_{11}$-G	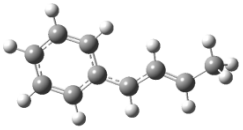	21	6.15	$D_1(A'')$←$D_0(A'')$	2.83 (437, ***474***)	0.0002
				$D_2(A'')$←$D_0(A'')$	3.22 (385)	0.0036
				$D_3(A'')$←$D_0(A'')$	3.68 (337)	0.0280

$C_{10}H_{11}$-H	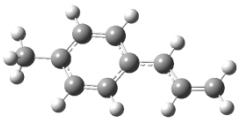	24	6.26	$D_1(A'')\leftarrow D_0(A'')$ $D_2(A'')\leftarrow D_0(A'')$ $D_3(A'')\leftarrow D_0(A'')$	2.82 (440, ***480***) 3.21 (387) 3.66 (339)	0.0018 0.0021 0.0195
$C_{10}H_{11}$-I	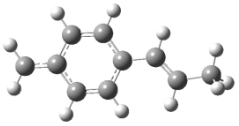	48	6.58	$D_1(A'')\leftarrow D_0(A'')$ $D_2(A'')\leftarrow D_0(A'')$ $D_3(A'')\leftarrow D_0(A'')$	2.53 (491, ***531***) 3.13 (396) 3.64 (341)	0.0043 0.0098 0.1088
$C_{10}H_{11}$-J	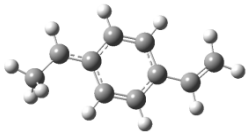	52	6.23	$D_1(A'')\leftarrow D_0(A'')$ $D_1(A'')\leftarrow D_0(A'')$ $D_1(A'')\leftarrow D_0(A'')$	2.53 (489, ***540***) 3.15 (394) 3.64 (340)	0.0001 0.0012 0.0751

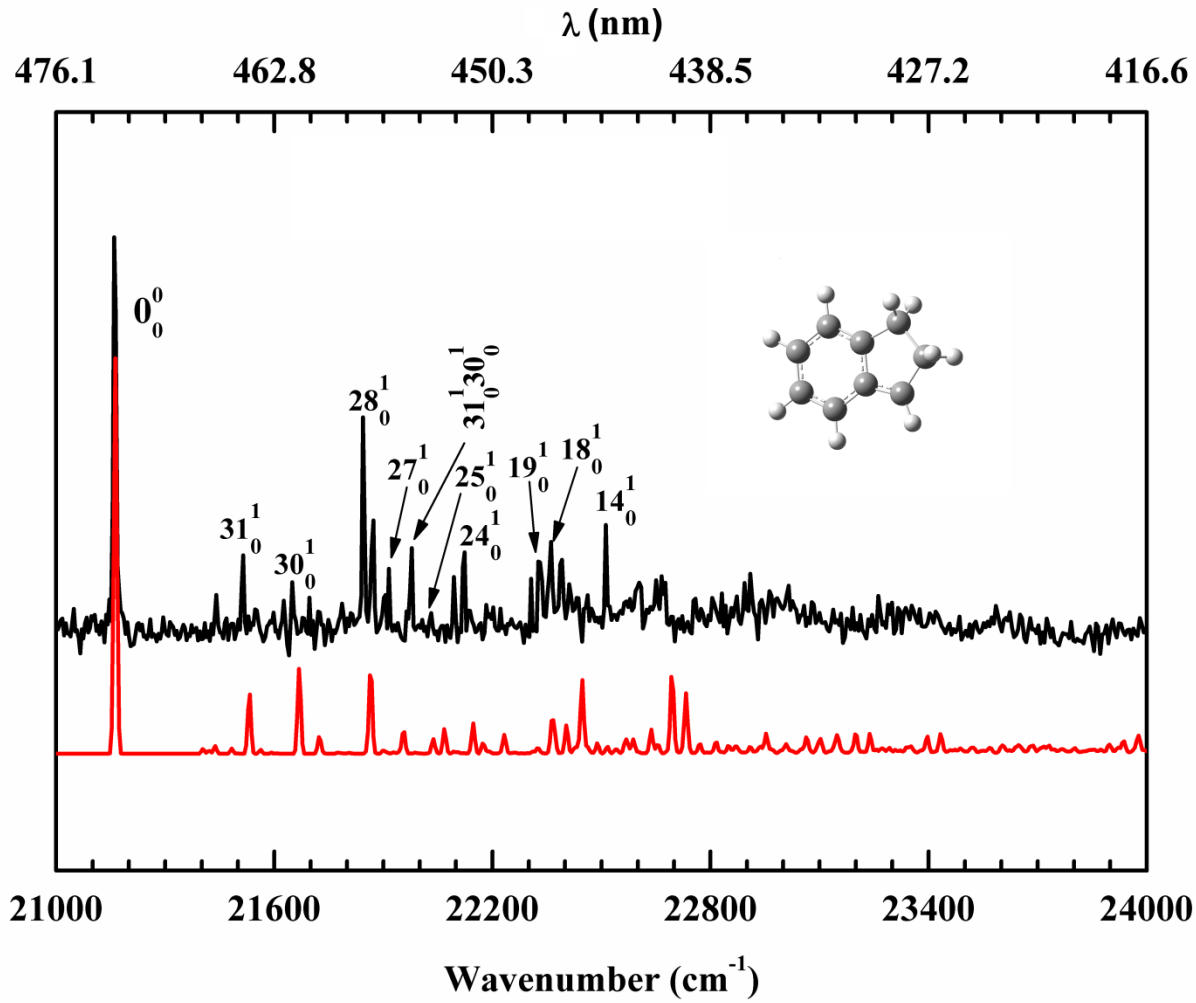

Figure 1. Resonant two-color two-photon ionization spectrum of 1-indanyl radical (C_9H_9; black trace) and the Franck-Condon simulation of the $D_1 \leftarrow D_0$ transition (red trace). Assignments are listed in Table 1.

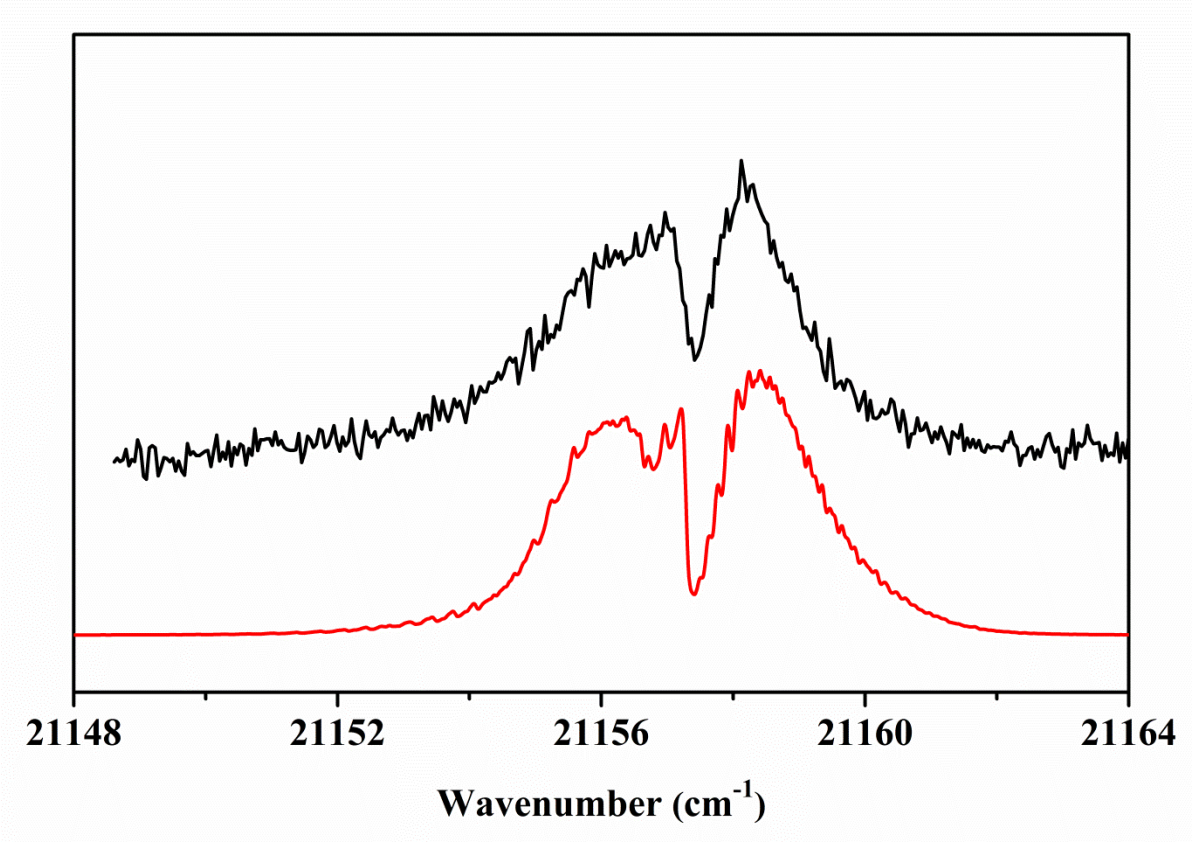

Figure 2. The origin band in the $D_1(A'')\leftarrow D_0(A'')$ electronic spectrum of 1-indanyl radical measured at a resolution of 0.08 cm^{-1} (black trace) and the simulated rotational contour at T=18K (red trace).

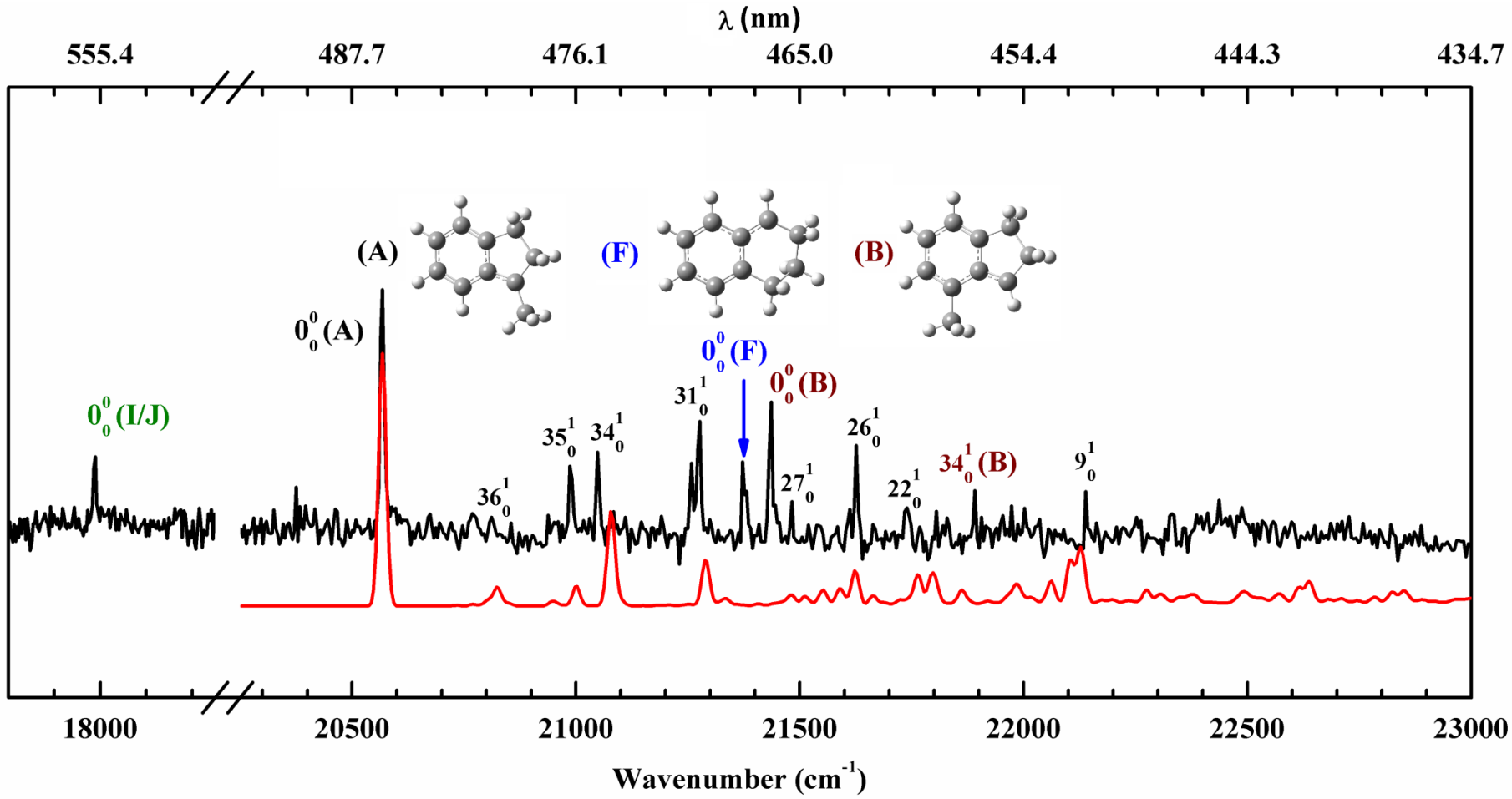

Figure 3. Resonant two-color two-photon ionization spectrum of $C_{10}H_{11}$ (black trace) and the Franck-Condon simulation of the $D_1 \leftarrow D_0$ vibrational pattern for isomer A (red trace). Assignments are listed in Table 2. Labeled transitions in black belong to isomer A.

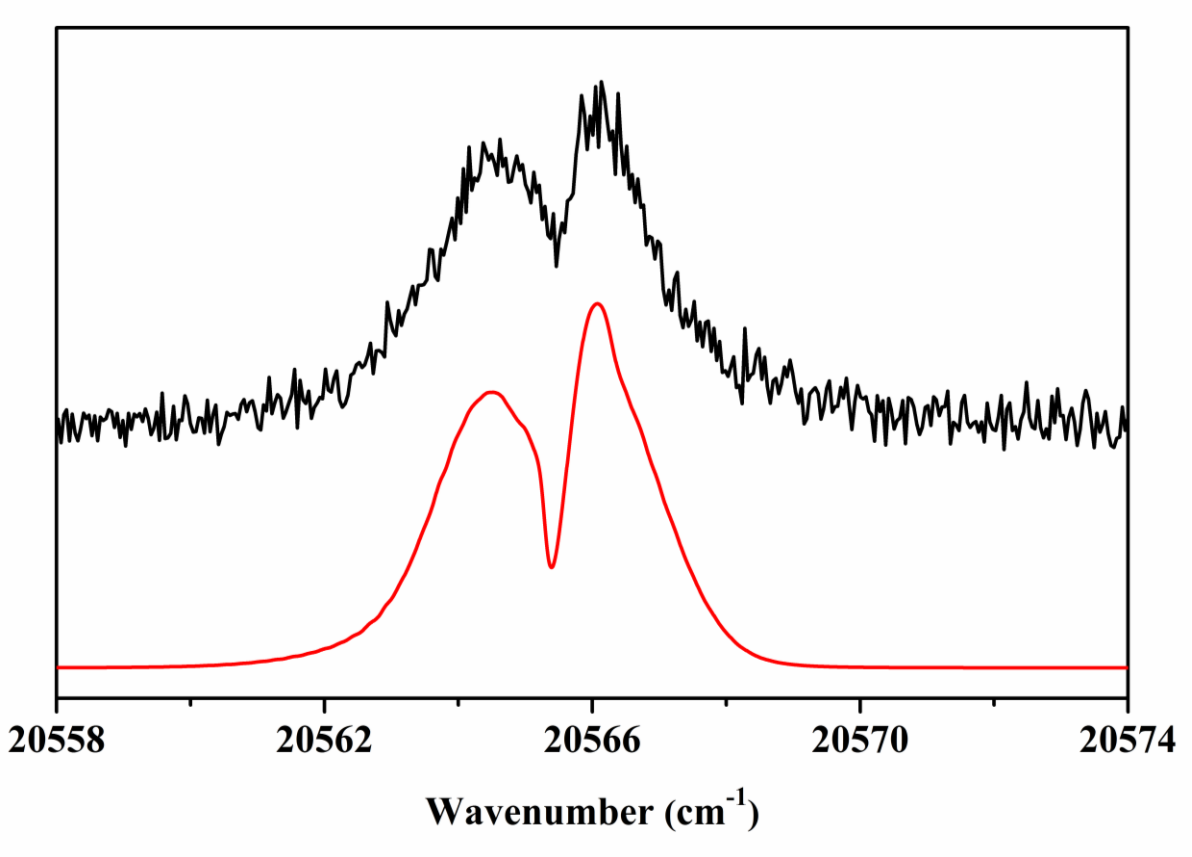

Figure 4. The origin band in the $D_1(A'')\leftarrow D_0(A'')$ electronic spectrum of isomer A (1-methyl-1-indanyl radical) measured at a resolution of 0.08 cm^{-1} (black trace) and the simulated rotational contour (red trace) at T=15K.